

Improving the efficiency of magnetic coupling energy transfer by etching fractal patterns in the shielding metals*

Qing-feng LI^{†1,2}, Shao-bo CHEN^{1,2}, Wei-ming WANG^{1,2}, Hong-wei HAO^{1,2}, Lu-ming LI^{†‡1,2,3}

(¹School of Aerospace, Tsinghua University, Beijing 100084, China)

(²National Engineering Laboratory for Neuromodulation, Beijing 100084, China)

(³Center of Epilepsy, Beijing Institute for Brain Disorders, Beijing 100084, China)

[†]E-mail: lqf05@mails.tsinghua.edu.cn; lilm@tsinghua.edu.cn

Received Apr. 9, 2015; Revision accepted Aug. 5, 2015; Crosschecked Dec. 8, 2015

Abstract: Thin metal sheets are often located in the coupling paths of magnetic coupling energy transfer (MCET) systems. Eddy currents in the metals reduce the energy transfer efficiency and can even present safety risks. This paper describes the use of etched fractal patterns in the metals to suppress the eddy currents and improve the efficiency. Simulation and experimental results show that this approach is very effective. The fractal patterns should satisfy three features, namely, breaking the metal edge, etching in the high-intensity magnetic field region, and etching through the metal in the thickness direction. Different fractal patterns lead to different results. By altering the eddy current distribution, the fractal pattern slots reduce the eddy current losses when the metals show resistance effects and suppress the induced magnetic field in the metals when the metals show inductance effects. Fractal pattern slots in multilayer high conductivity metals (e.g., Cu) reduce the induced magnetic field intensity significantly. Furthermore, transfer power, transfer efficiency, receiving efficiency, and eddy current losses all increase with the increase of the number of etched layers. These results can benefit MCET by efficient energy transfer and safe use in metal shielded equipment.

Key words: Fractal pattern, Metal-layer-shield, Eddy current, Magnetic coupling energy transfer
<http://dx.doi.org/10.1631/FITEE.1500114>

CLC number: TN99

1 Introduction


Magnetic coupling energy transfer (MCET) is one of the most active research fields nowadays. Magnetic coupling resonance has been proposed as a way to increase energy transfer distance as a milestone in MCET (Kurs *et al.*, 2007). This progress has drawn great attention from scientists and industry personnel. The Wireless Power Consortium (WPC) released the first wireless charging standard, Qi, in 2010, and has attracted 211 member organizations from 20 countries. There are already 638 Qi-certified products available. In addition, many communication

equipment manufacturers (e.g., Apple, Samsung, and Qualcomm) and car manufacturers (e.g., Toyota, Nissan, and Volvo) have started the MCET research. Apple Inc. applied for 12 patents about the topic from 2007 to 2011. Besides, medical device manufacturers including Medtronic, St. Jude, and Boston Scientific have released rechargeable spinal cord stimulators (SCSs). Medtronic released the world's first rechargeable deep brain stimulator (DBS), Activa RC, in 2009. MCET is promising in various applications such as mobile consumer electronics, electric vehicles, and active implantable medical devices (Ye *et al.*, 2008; Ho *et al.*, 2014), and is a huge potential emerging industry.

However, the thermal budgets of the wireless charging devices are always tight, especially in implantable medical applications. A major heat source comes from the unintended eddy currents in metal

[‡] Corresponding author

* Project supported by the National Natural Science Foundation of China (No. 51125028) and the National Key Technology R&D Program of China (No. 2011BAI12B07)

 ORCID: Qing-feng LI, <http://orcid.org/0000-0002-8827-8511>

© Zhejiang University and Springer-Verlag Berlin Heidelberg 2016

objects. These metal objects include the inner copper layers of printed circuit boards (PCBs) and the metal cases of mobile electronics, electric vehicles, and implantable medical devices. These metals are often located in the coupling region of MCET systems. It makes the optimal design of MCET systems very difficult, reduces the energy transfer efficiency, and increases device heating. The metal objects affect the mutual inductance, self-inductance, and effective series resistance of the coils (Geselowitz *et al.*, 1992), making the design optimization complex and difficult. To minimize the influence of the metals, the use of ETD-core coils (Albesa and Gasulla, 2012) and low frequency carriers (Zangl *et al.*, 2010) was proposed. Yu *et al.* (2013) re-optimized the coil size and the resonant capacitor and placed another metal plate in a symmetrical way to compensate for the impacts of a metal plate. However, these approaches are often restricted by the size, structure, material, and variable coupling conditions in a practical implementation. Thus, the transfer power is still not high enough in a metal shielded environment. Accordingly, the Qi standard currently applies only to the transfer of power around 15 W. Lovik *et al.* (2011) tested rechargeable SCSs from Medtronic, St. Jude, and Boston Scientific and found that the devices all had heating problems. Furthermore, St. Jude received three reports of skin surface burns (one second-degree and two first-degree burns) believed to be associated with heating during charging the Eon and Eon Mini devices.

Suppressing the eddy currents in the metals is an effective way to improve the transfer efficiency and the device security. The conductivity, the thickness, the area and shape factor of a metal sheet, the intensity and frequency of the magnetic field all affect the eddy current losses (Siakavellas, 1997). However, due to practical limitations, the conductivity, thickness, and area of the metal sheet, and the intensity and frequency of the magnetic field cannot be easily optimized to reduce the losses. Fractal geometries are promising in solving certain electromagnetic problems. Different from Euclidean geometries, fractal geometries are unique for their self-similarity, space-filling properties, and aesthetic characteristics, which have attracted a lot of interest (Kufa and Raida, 2013; Rani and Singh, 2013). We propose to etch fractal patterns in the metals to change the metals'

shape factors and suppress the eddy currents. This promising approach will improve the transfer efficiency and the safety.

This study investigates how to improve the MCET efficiency by etching fractal patterns in metals. Four parameters are used to evaluate the MCET performance: transfer power (P_T), transfer efficiency (η), eddy current losses (P_E), and receiving efficiency (P_T/P_{TR}). Here, P_{TR} is the total received power including eddy current losses, receiving coil losses, and the transferred power, so the receiving efficiency reflects the losses for a given transfer power (P_T). These four parameters are also used to evaluate the abilities of the fractal patterns to suppress the eddy currents. Various fractal patterns are investigated and the mechanisms are analyzed for single and multiple metal layers. These results are also verified experimentally.

2 Simulation

CST EM STUDIO 2012 is used to examine which features of the patterns can effectively suppress the eddy currents. Several fractal patterns satisfying these features are proposed to identify the best pattern. The suppressing mechanism is analyzed based on the results for the best pattern for frequencies from 1 to 1000 kHz. The eddy currents in multilayer metal structures are also investigated.

2.1 Simulation model

The model to simulate the condition with the metal-layer shielded is shown in Fig. 1. To mimic the use of MCET in mobile electronics and some medical implants such as SCS and DBS, the model uses a circular transmitting coil with a rectangular cross-section. The coil has an inner diameter of 40 mm, an outer diameter of 50 mm, and a thickness of 5 mm, while the circular receiving coil has an inner diameter of 40 mm, an outer diameter of 50 mm, and a thickness of 2 mm. A magnetic core (R2KB1, relative permeability 2300, 38 mm diameter, and 5 mm height) is placed in the transmitting coil. The coils are coaxially aligned. The distance between the coils is 10 mm. A circular metal sheet (titanium, conductivity 1.8×10^6 S/m) 100 mm in diameter and 0.3 mm in thickness is placed between the coils. A current

source of 1 A amplitude and 10 kHz frequency is used as the source with a 100 Ω resistor as the load.

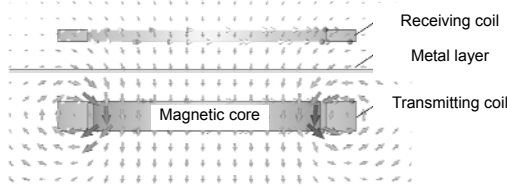


Fig. 1 Simulation model

2.2 Features of patterns effectively suppressing the eddy currents

The eddy currents in the metal sheet flow in circular paths, so radial slots can suppress the eddy currents. The key pattern features that suppress the eddy currents were studied by using three etching schemes (Figs. 2a–2c). Various slots' distances L and depths h were analyzed to give the results (Fig. 3).

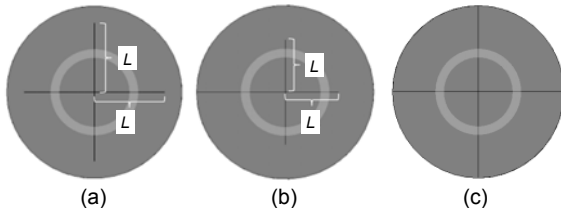


Fig. 2 Three etching schemes for the metal sheet

(a) Four 0.3 mm deep slots begin at the disk center and end at a distance L from the center; (b) Three 0.3 mm deep slots begin at the disk center and end at a distance L from the center with a fourth slot ending at the disk boundary; (c) The slots all extend to the edge with varying slot depth h . All the slots have a fixed 0.3 mm width

As shown in Figs. 3a and 3b, for the scheme in Fig. 2a, P_T , η , and P_T/P_{TR} significantly increase while P_E is reduced for slot length L larger than 20 mm. The eddy currents are suppressed the most when the slots end at the boundary ($L=50$ mm) with P_E reduced to 0.95 W (7.21 W before etching). For the scheme in Fig. 2b, P_E is reduced to 0.99 W when $L=20$ mm (Fig. 3d). The results in Figs. 3a–3d show that the scheme in Fig. 2b provides the same eddy current suppression with a shorter total slot length than the scheme in Fig. 2a. The only difference between the two schemes is the slot ending at the disk boundary in Fig. 2b, so interrupting the metal surface at the edge is probably a key feature of the patterns that effectively suppress the eddy currents.

The results in Fig. 3d show that P_E is not reduced much more when L is larger than 20 mm. Noting that the transmitting coil radius is only 20 mm, the high-intensity magnetic field region in the metal is in the area with $L \leq 20$ mm. Thus, the patterns should be etched in the high-intensity magnetic field region as the second feature.

The scheme in Fig. 2c satisfies both of these features, but P_E is reduced only when $h=0.3$ mm, as shown in Fig. 3f. Thus, the metal should be etched through completely as the third key feature.

In summary, slots etched in the metals can suppress the eddy currents. The slots which can effectively suppress the eddy currents should reach the metal edge, be etched in the high-intensity magnetic field region, and pass completely through the metal.

2.3 Different slot fractal patterns

Several slot fractal patterns satisfying the key features given in Section 2.2 are shown in Fig. 4. The parameters of η , P_E , and the suppression efficiency were analyzed to find the best pattern. The suppression efficiency is defined as the percentage of the reduction of P_E per millimeter of slot length. When the goal is to improve η , η is normalized against the result with no metals; when the goal is to reduce P_E or improve the suppression efficiency, the result is normalized against that with a metal sheet having no slots. The normalized results are shown in Table 1.

The transfer efficiencies, η , in schemes in Fig. 4a, 4c–4e, 4g, and 4h are all more than 90%, which means that the influence of the metal on MCET can be almost neglected when the goal is to improve η . When the goal is to reduce P_E , schemes in Figs. 4e, 4g, and 4h all reduce P_E to less than 10%. Assuming 0.30%/mm is an acceptable suppression efficiency, schemes in Figs. 4a, 4c, 4d, 4f, and 4g are all satisfactory. Therefore, the scheme in Fig. 4g is considered to be the best pattern which satisfies all the goals.

2.4 Mechanism of suppressing eddy current effects by slot fractal patterns

The eddy currents influence the MCET performance by means of the eddy current losses and the induced magnetic field shielding. Therefore, the metal sheets can be treated as an equivalent resistor (R), connected with a serial equivalent inductor (L). This model can be described by Eq. (1):

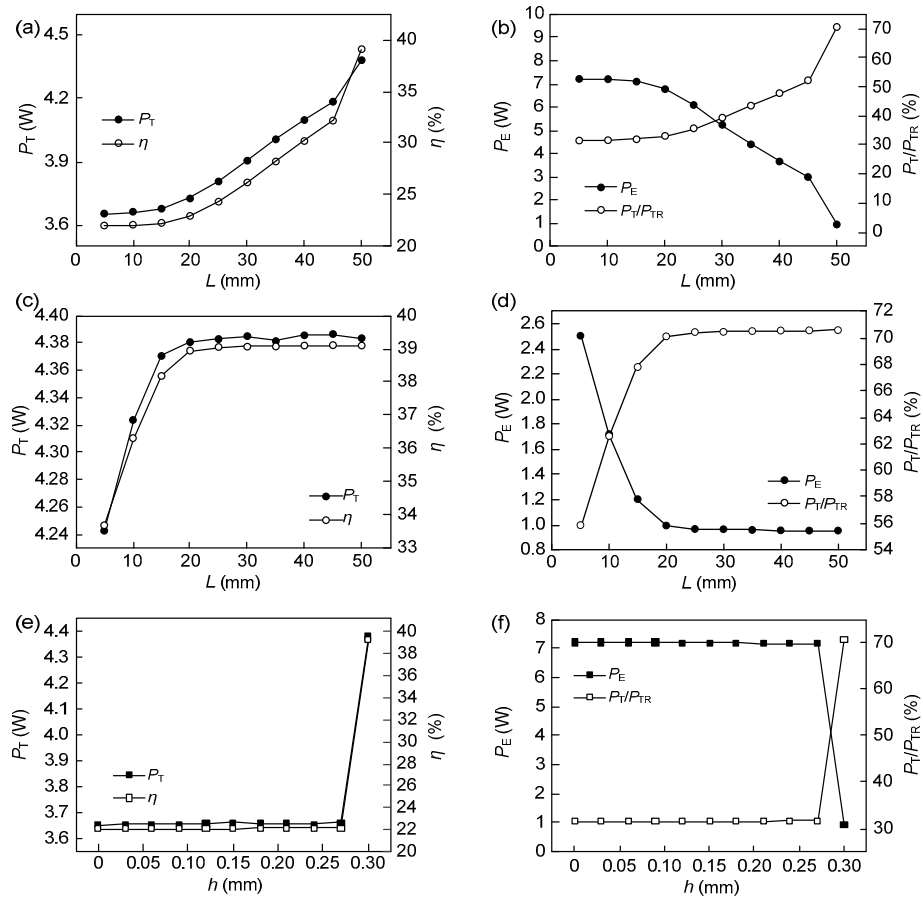


Fig. 3 Simulation results for the patterns in Fig. 2

(a) Results of P_T and η for the pattern in Fig. 2a; (b) Results of P_E and P_T/P_{TR} for the pattern in Fig. 2a; (c) Results of P_T and η for the pattern in Fig. 2b; (d) Results of P_E and P_T/P_{TR} for the pattern in Fig. 2b; (e) Results of P_T and η for the pattern in Fig. 2c; (f) Results of P_E and P_T/P_{TR} for the pattern in Fig. 2c

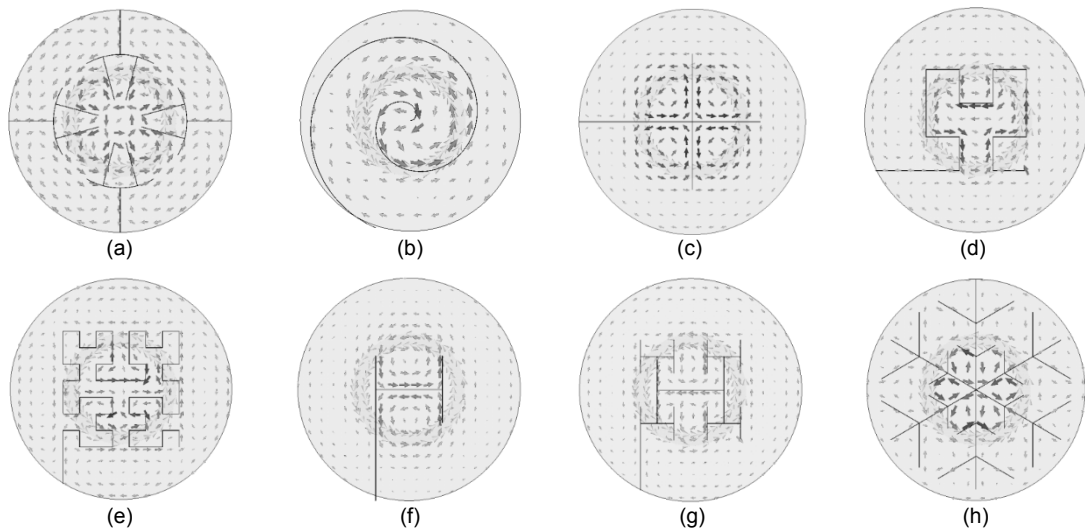


Fig. 4 Slot fractal patterns

(a) Tree fractal; (b) Helical fractal; (c) Cross fractal; (d) Hilbert fractal with order two; (e) Hilbert fractal with order three; (f) H-shaped fractal with order one; (g) H-shaped fractal with order two; (h) Snow fractal. The arrows in the metal sheet represent the flow direction of the eddy currents

Table 1 Results for different slot fractal patterns in Fig. 4

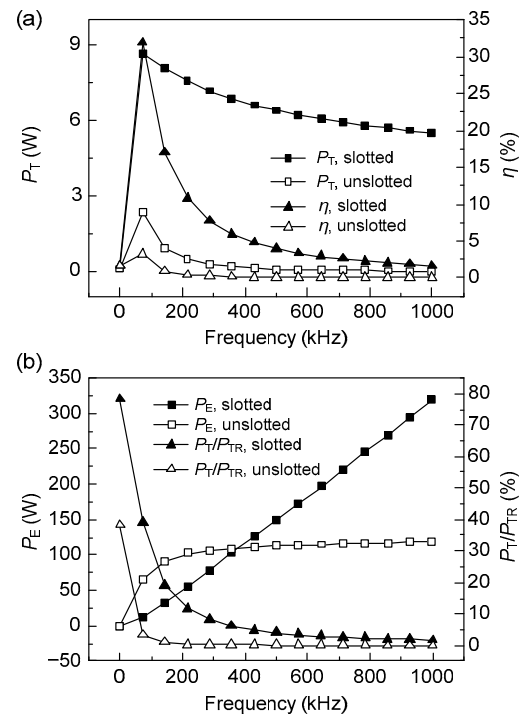
Scheme	P_E (%)	P_T (%)	η (%)	P_T/P_{TR} (%)	Slots length (mm)	Suppression efficiency (%/mm)
Fig. 4a	10.1	98.7	92.8	88.0	245.66	0.366
Fig. 4b	23.9	96.6	84.1	74.7	280.88	0.271
Fig. 4c	13.3	98.2	90.7	84.3	140.00	0.619
Fig. 4d	11.5	98.4	91.8	86.7	247.50	0.357
Fig. 4e	4.0	99.6	97.1	95.2	489.25	0.196
Fig. 4f	16.6	97.5	88.5	81.9	125.00	0.667
Fig. 4g	6.5	99.1	95.3	92.8	292.50	0.320
Fig. 4h	3.5	99.6	97.4	96.4	635.00	0.152
No slot	100.0	81.8	51.1	38.6	Null	Null
No metal	Null	100.0	100.0	100.0	Null	Null

$$L \frac{di(t)}{dt} + Ri(t) = \varepsilon(t), \quad (1)$$

where $\varepsilon(t)$ is the electromotive force induced in the metal sheet. The metal sheets show mainly resistance effects when the conductivity or the frequency is low enough and inductance effects when the conductivity or the frequency is high. When the metal sheets show mainly resistance effects, an increasing frequency will lead to larger induced voltages $\varepsilon(t)$ and thus increased losses. Similarly, when the metal sheets show mainly inductance effects, due to the unchanged eddy currents $i(t)$, an increasing frequency will not change the losses when the metal is thinner than the skin depth or will slightly reduce the losses when the metal is thicker than the skin depth.

The suppressing mechanism of the slot fractal patterns was investigated over a relatively wide frequency range of 1 to 1000 kHz (Fig. 5) for the pattern in Fig. 4g. P_T , η , and P_T/P_{TR} are all improved over the whole frequency range. P_E is reduced at frequencies below 400 kHz with the slots but increases at high frequencies. Furthermore, P_E increases with frequencies from 400 to 1000 kHz, which indicates that the metal layer behaves like a resistor instead of an inductor.

For the patterns in Fig. 4, the longer eddy current path in the metal sheet after slotting suggests that the equivalent resistance increases. The eddy currents on the two sides of the slots flow in opposite directions, suggesting that the equivalent inductance decreases. Based on Eq. (1), the slot fractal pattern reduces the eddy current losses, P_E , with mainly the resistance effect at low frequencies, and suppresses the induced magnetic field shielding due to the inductance effect at high

**Fig. 5 Frequency responses with the slot fractal pattern in Fig. 4g: (a) P_T and η ; (b) P_E and P_T/P_{TR}**

frequencies. This mechanism improves all of P_T , η , and P_T/P_{TR} . The eddy current effect at high frequencies changes to resistive, which leads to a larger P_E .

2.5 Suppressing eddy current effects in multilayer metal sheets

Multilayer metal sheets are very common in MCET applications due to the wide use of multilayer PCBs and metal cases. In some MCET applications, such as underwater and transcutaneous energy transfer, metal cases are often used to seal the energy receiving parts. Slots cannot be etched in these cases.

However, slots can be etched in the PCB copper layers. This section investigates suppressing the eddy currents to improve the MCET performance by etching slot fractal patterns in the PCB copper layers.

In this section, the metal case is represented by a titanium board (conductivity 1.8×10^6 S/m, thickness 0.3 mm) since the metal with low conductivity will lead to a higher transfer efficiency. The receiving coil is placed above the PCB copper layers (two layers, conductivity 6×10^7 S/m, thickness 0.036 mm), as shown in Fig. 6. The results in Table 2 are obtained using the fractal pattern in Fig. 4g to etch the copper layers and the data is normalized against the results with no copper.

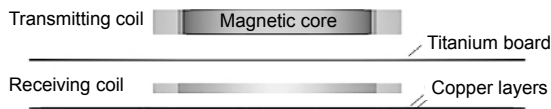


Fig. 6 Model for suppressing eddy currents in three metal layers

Table 2 Eddy current suppression in three metal layers

Scheme	P_E (%)	P_T (%)	η (%)	P_T/P_{TR} (%)
No copper	100.0	100.0	100.0	100.0
No slot	88.1	34.2	44.3	50.0
Etching one layer	99.9	46.0	53.7	56.3
Etching two layers	103.7	94.0	94.0	93.8

As shown in Table 2, the copper layers lead to worse MCET performances with $P_T=34.2\%$, $\eta=44.3\%$, and $P_T/P_{TR}=50.0\%$. The copper layers reduce P_E to 88.1%, suggesting that the copper layers have an inductive effect which reduces the magnetic field strength in the titanium board. The slot fractal pattern reduces the induced magnetic field intensity in the copper layers and thus improves P_T , η , and P_T/P_{TR} but increases P_E . Furthermore, P_T , η , P_E , and P_T/P_{TR} all increase with the increase of the number of etched layers. The MCET performance after etching the slots in all the copper layers is almost the same as that with no copper, suggesting that the influence of the copper layers can be ignored after etching the slots.

In summary, the PCB copper layers often affect the MCET performance with inductive effects due to their high conductivity. The slot fractal patterns in the copper layers can suppress the copper induced magnetic field and significantly improve the MCET performance.

3 Experiments

The fractal pattern in Fig. 4g was investigated experimentally to verify the features of the patterns that effectively suppress the eddy currents in single and multiple metal layers.

3.1 Experimental platform

The experimental platform is shown in Fig. 7. The power of the excitation source and the current in the transmitting coil were recorded by a power analyzer (Voltech PM 1000+, UK). The load voltage was measured with an oscilloscope (Tektronix MSO4104 with voltage probe P6319A, US) and then used to calculate the transfer power, P_T . A signal generator (SP SPF40, China) and a power amplifier (NF HSA4012, Japan) were used to excite the transmitting coil at 10 kHz. Fig. 8 shows the coils and the metal samples. A high permeability core (R2KB1) was placed in the transmitting coil. The PCB copper disks were all 0.036 mm thick. The titanium board was 0.3 mm thick. A 100 Ω resistor was used as the load.

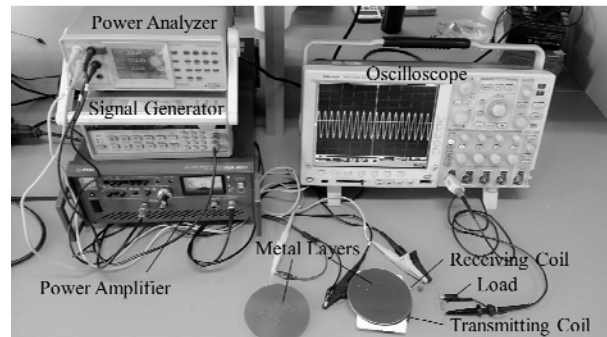


Fig. 7 Experimental platform

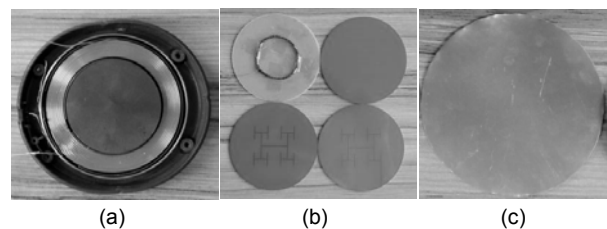


Fig. 8 The coils and the metal samples

(a) Transmitting coil; (b) Receiving coil, PCB copper disk without slots, PCB copper slotted disk without breaking the edge, and PCB copper slotted disk to the edge (from left to right and from top to bottom); (c) Titanium board

3.2 Features of patterns effectively suppressing the eddy current effects

The MCET performance was evaluated for the four test conditions shown in Fig. 9. P_T , η , and P_T/P_{TR} were normalized to the no metal condition as the reference while P_E was normalized to the no slot condition as the reference.

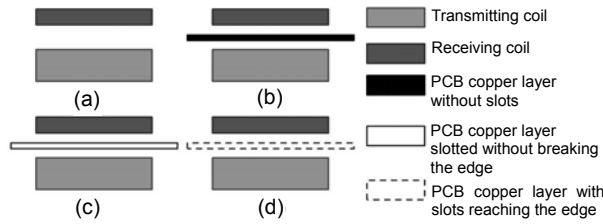


Fig. 9 Four experimental designs for evaluation of slots' key pattern features

(a) No metal is presented between the transmitting coil and the receiving coil; (b) A PCB copper layer without slots is present between the coils; (c) A PCB copper layer slotted without breaking the edge is present between the coils; (d) A PCB copper layer with slots reaching the edge is present between the coils

As shown in Table 3, with these etched slots, the influence of the copper can be ignored with $P_T=95.8\%$ and $\eta=86.2\%$ for the scheme in Fig. 9d, which suggests that the etched slots effectively suppress the eddy currents. In addition, the best results are obtained when the metal edge is broken, since the improvement of the MCET performance is little for the scheme in Fig. 9c but significant for the scheme in Fig. 9d with the results for the scheme in Fig. 9b as the reference.

Table 3 Results for the four conditions in Fig. 9

Scheme	P_E (%)	P_T (%)	η (%)	P_T/P_{TR} (%)
Fig. 9a	0	100.0	100.0	100.0
Fig. 9b	100.0	64.7	20.6	8.7
Fig. 9c	79.0	75.2	27.9	12.4
Fig. 9d	6.7	95.8	86.2	72.0

In summary, the experiments verified that the etching of fractal pattern slots in the metal layers effectively suppresses the eddy current effects and that the slots must reach the metal edge.

3.3 Suppressing eddy current effects in multiple metal layers

The MCET performance was evaluated for the

four test conditions as shown in Fig. 10. The results were normalized to the no copper condition (Fig. 10a) as the reference. The comparisons between the results of simulation and experiment are shown in Fig. 11.

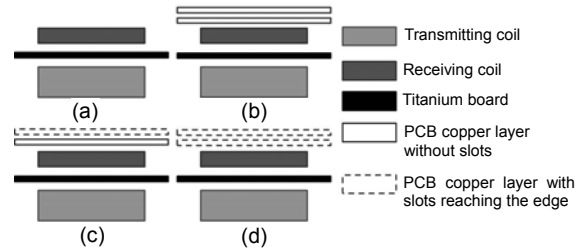


Fig. 10 Suppressing eddy current effects of slots in multiple metal layers

(a) A titanium board is present between the transmitting coil and the receiving coil; (b) Two additional PCB copper layers are present above the receiving coil; (c) Two additional PCB copper layers with one layer slotted are present above the receiving coil; (d) Two additional PCB copper layers with both layers slotted are present above the receiving coil

The simulation results for the variation trends of P_T , η , and P_T/P_{TR} for the four conditions are consistent with the experimental results. The eddy current losses in Fig. 11 contain two parts, the losses in the titanium board and the losses in the PCB copper layers. The copper layers act as inductors that reduce the magnetic field intensity in the titanium board since the eddy current losses, P_E , in the scheme in Fig. 10b are less than those with no copper (scheme in Fig. 10a). P_T , η , and P_T/P_{TR} all increase with an increasing number of slotted copper layers. The etched slots reduce the magnetic field intensity decrease caused by the copper layers, which improves P_T , η , and P_T/P_{TR} . However, the slots lead to higher losses in the titanium board. With the addition of the losses in the copper layers, the total eddy current loss in the scheme in Fig. 10d is the highest. The etching of proper slots in all the copper layers essentially eliminates the influence on the MCET performance with P_T , η , and P_T/P_{TR} all more than 90%. Actually, the parameter P_E in Fig. 11 is possible to be larger than 100%, while the others are not. However, slight positional misalignment of the coils, the titanium board, and the PCB copper layers is inevitable in the experiments, which leads to errors in the results. The energy transfer performance in the scheme in Fig. 10d is approximately equal to that in the scheme in Fig. 10a. The errors may cause the experimental results of

P_T , η , and P_T/P_{TR} in the scheme in Fig. 10d to be larger than 100%.

The experimental results are consistent with the simulation results, which verify that the proper fractal pattern slots can reduce the induced magnetic field strength in the copper layers to significantly improve the MCET performance. Moreover, the performance can be improved better with more etched layers.

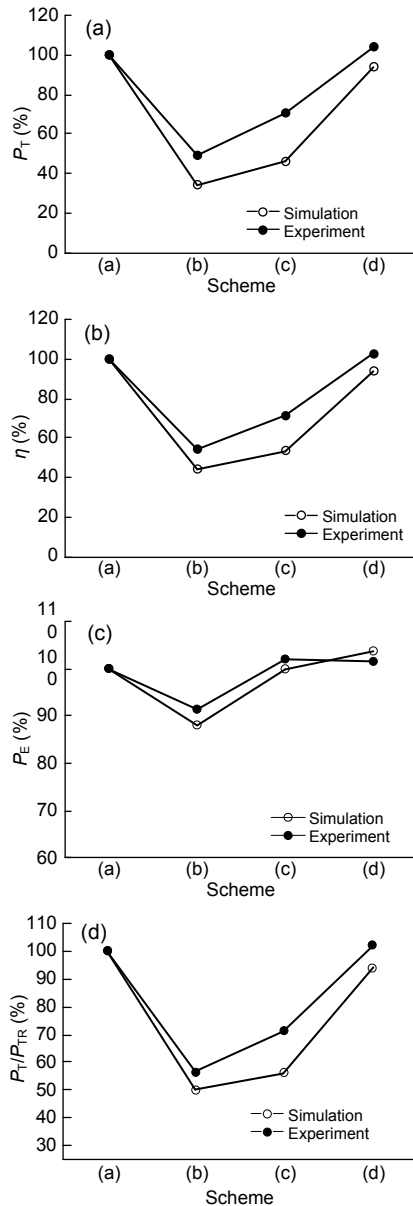


Fig. 11 Comparisons of simulation and experimental results in Fig. 10

(a) Comparison of P_T ; (b) Comparison of η ; (c) Comparison of P_E ; (d) Comparison of P_T/P_{TR}

4 Discussion

4.1 Effective etching approach for suppressing eddy current effects

The results in Fig. 3 and Table 3 show that the slot fractal patterns in the metal layers for suppressing the eddy currents should reach the metal edge, be etched in the main magnetic field region, and be etched completely through the metal layers. As shown in Fig. 12, slots that break the metal edge greatly disturb the original circular patterns of the eddy currents. From a topology view, breaking the edge maintains the simple connectivity of the metal sheet. Further, the patterns in Fig. 4 all keep the simple connectivity of the original plane and effectively suppress the eddy currents. Fig. 12c shows that the eddy current distribution changes little when the metal is not etched deep enough, although the simple connectivity of the plane is kept. Therefore, maintaining the simple connectivity of the metal plane and etching completely through the metal surface are the essential requirements for suppressing the eddy currents by etching patterns in the metals.

4.2 Errors analysis

As shown in Fig. 11, the variation trends in P_T , η , and P_T/P_{TR} in the experiments are consistent with those in simulations. Some errors in specific values may be due to four factors. First, the titanium board used in the experiments is not perfectly flat, which could cause slight changes in the eddy current distributions. Second, the presence of impurities in the metals would lower the conductivities of the titanium and the copper, which would reduce the magnetic field shielding effects and give higher transfer

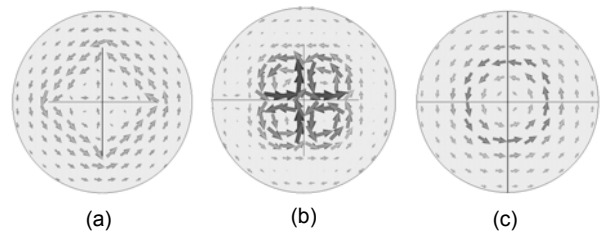


Fig. 12 Eddy current distribution shapes in Fig. 2

(a) Eddy current distribution in Fig. 2a with $L=20$ mm; (b) Eddy current distribution in Fig. 2b with $L=20$ mm; (c) Eddy current distribution in Fig. 2c with $h=0.2$ mm. The arrows in the figures represent the eddy currents directions in the metal sheet

efficiencies, transfer powers, and receiving efficiencies than those in the simulation results. Third, the numerical calculations could have some errors due to cutting off of the calculation region and the data. Finally, slight misalignments could cause further errors since the MCET system is very sensitive to the coupling position. All these factors will contribute to the errors; however, the largest error in P_E is less than 4%, which is acceptable.

4.3 Optimizing the fractal patterns

As shown in Table 1, different fractal patterns lead to different results. A future work will be finding the optimum pattern for a given metal layer. The optimization can be divided into optimizing the pattern parameters and optimizing the pattern topology. The pattern parameters can be easily optimized through a sensitivity analysis. Optimizing the pattern topology is more difficult since the fractal theory has not been fully established and using fractal geometry to solve electromagnetic problems in such applications has begun lately. The fractal pattern topology should be optimized for more complex metal environments. This work will promote fractal theory applications in electromagnetics.

4.4 Magnetic field regulation approach

High conductivity metals are commonly used in practical applications to shield against external magnetic fields. However, when a high intensity magnetic field is desired in some areas, the metal structure must be optimized. This paper has shown that fractal pattern slots can alter the eddy current distribution and suppress the induced magnetic shielding. Furthermore, precise magnetic field regulation is possible if the pattern topology can be optimized. Thus, fractal pattern slots in metals can be used to regulate magnetic fields.

5 Conclusions

Fractal patterns can be etched in metal surfaces to suppress eddy currents. This study investigated the use of fractal slots to effectively suppress eddy

currents. Various fractal patterns were analyzed and the mechanisms were investigated to provide an approach to suppress eddy currents in multiple metal layers. This work described an effective way to suppress the eddy currents and promoted MCET applications in metal-layer-shielded environments.

References

- Albesa, J., Gasulla, M., 2012. Inductive power transfer for autonomous sensors in presence of metallic structures. *IEEE Int. Instrumentation and Measurement Technology Conf.*, p.664-669.
<http://dx.doi.org/10.1109/I2MTC.2012.6229658>
- Geselowitz, D.B., Hoang, Q.T.N., Gaumond, R.P., 1992. The effects of metals on a transcutaneous energy transmission system. *IEEE Trans. Biomed. Eng.*, **39**(9):928-934.
<http://dx.doi.org/10.1109/10.256426>
- Ho, J.S., Yeh, A.J., Neofytou, E., et al., 2014. Wireless power transfer to deep-tissue microimplants. *PNAS*, **111**(22): 7974-7979. <http://dx.doi.org/10.1073/pnas.1403002111>
- Kufa, M., Raida, Z., 2013. Lowpass filter with reduced fractal defected ground structure. *Electron. Lett.*, **49**(3):199-201.
<http://dx.doi.org/10.1049/el.2012.3473>
- Kurs, A., Karalis, A., Moffatt, R., et al., 2007. Wireless power transfer via strongly coupled magnetic resonances. *Science*, **317**(5834):83-86.
<http://dx.doi.org/10.1126/science.1143254>
- Lovik, R.D., Abraham, J.P., Sparrow, E.M., 2011. Surrogate human tissue temperatures resulting from misalignment of antenna and implant during recharging of a neuromodulation device. *Neuromodulation*, **14**(6):501-511.
<http://dx.doi.org/10.1111/j.1525-1403.2011.00396.x>
- Rani, S., Singh, A.P., 2013. Modified Koch fractal antenna with asymmetrical ground plane for multi and UWB applications. *Int. J. Appl. Electrom.*, **42**(2):259-267.
<http://dx.doi.org/10.3233/JAE-131662>
- Siakavellas, N.J., 1997. Two simple models for analytical calculation of eddy currents in thin conducting plates. *IEEE Trans. Magn.*, **33**(3):2245-2257.
<http://dx.doi.org/10.1109/20.573839>
- Ye, D.D., Yan, G.Z., Wang, K.D., et al., 2008. Development of a non-cable whole tectorial membrane micro-robot for an endoscope. *J. Zhejiang Univ.-Sci. A*, **9**(8):1141-1149.
<http://dx.doi.org/10.1631/jzus.A0720074>
- Yu, X., Skauli, T., Skauli, B., et al., 2013. Wireless power transfer in the presence of metallic plates: experimental results. *AIP Adv.*, **3**(6):062102.
<http://dx.doi.org/10.1063/1.4809665>
- Zangl, H., Fuchs, A., Bretterklieber, T., et al., 2010. Wireless communication and power supply strategy for sensor applications within closed metal walls. *IEEE Trans. Instrum. Meas.*, **59**(6):1686-1692.
<http://dx.doi.org/10.1109/TIM.2009.2026602>